Global NEST Journal, **28** (8), 08506
Available online: 27/08/2026

Optimizing the electro-Fenton treatment of sulfamethazine: Statistical modeling, mineralization kinetics, and energy consumption

Dorsaf Mansour[1]*, Abdulmohsen Khalaf Dhahi Alsukaibi[1], Souhaila Trabelsi Souissi[2], Faiza I.A. Abdella[1], Walaa I El-Sofany[1], Nizar Bellakhal[3] and Abdeltif Amrane[4]

[1]Chemistry Department, College of Sciences, University of Ha'il, Hail 55476, Saudi Arabia
[2]Tunis El Manar University, El Manar Preparatory Institute for Engineering Studies, P.O. Box 248, Tunis 2092, Tunisia
[3]Laboratory of Eco-Chimie, National Institute of Applied Sciences & Technology, P.O. Box 676, Tunis 1080, Tunisia
[4]Université de Rennes 1, Ecole Nationale Supérieure de Chimie de Rennes, CNRS, UMR 6226, 11 allée de Beaulieu, CS 50837, 35708 Rennes Cedex 7, France

*Correspondence e-mail: d.mansour@uoh.edu.sa

Abstract

This work focuses on optimizing of operating conditions of the electro-Fenton process for a clean and efficient elimination of sulfamethazine, a persistent antibiotic frequently detected in wastewater. The study examined the effects of experimental parameters, including current intensity, electrolysis duration and ferrous ion concentration, as well as their interactions, using response surface methodology based on a Doehlert experimental design. The results indicated that under specific conditions (0.5 mM ferrous ions, 0.5 A, 50 mM sodium sulfate, at pH 3), a 90% mineralization of 0.2 mM sulfamethazine was achieved. A statistically significant quadratic polynomial model was developed and validated through an analysis of variance (ANOVA). Statistical evaluation yielded a determination coefficient (R2) of 0.986, alongside a p-value of $p < 0.001$. These metrics establish the statistical significance of the regression, thereby validating its predictive accuracy within the defined experimental domain. The energy consumption of this system was determined to be 1.2 kilowatt-hours per gram of total organic carbon (TOC) removed. Additionally, the short-chain carboxylic acids and inorganic ions produced were quantified and monitored throughout the treatment process. Due to its high durability and efficiency, the electro-Fenton method is regarded as a promising technology for wastewater treatment.

Keywords: Electro-Fenton; Sulfamethazine; Doehlert matrix; Mineralization kinetics; Response surface methodology.

OPEN ACCESS

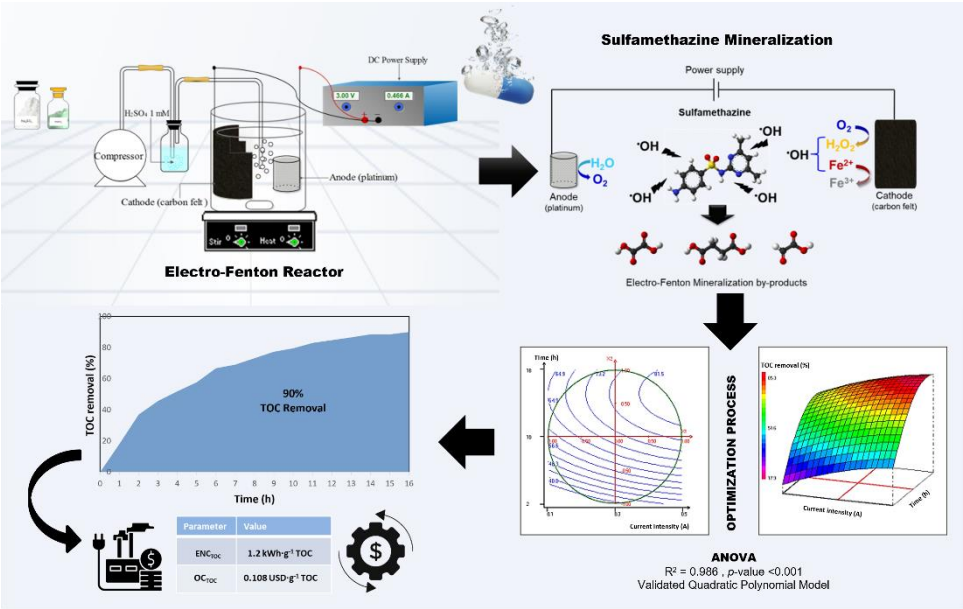
Received: 10/03/2026,

Accepted: 27/08/2026,

Available online: 27/08/2026

Copyright: © 2026 The Author(s). Published in Global NEST Journal. This article is licensed under the terms and conditions of the Creative Commons Attribution 4.0 International license (CC BY 4.0).

Graphical abstract



1. Introduction

A notable increase in the concentration of pharmaceutical compounds has been observed in surface water, groundwater, and partially treated wastewater over the last decade (Fallah *et al.* 2021; Latif *et al.* 2023; Hrkal and Pastuszek 2023; Yin *et al.* 2023). According to the World Health Organization (WHO) in 2012 (World Health Organization 2012), these substances are typically found at low concentrations in wastewater, generally below 0.1 $\mu g \cdot L^{-1}$, while treated water contains even lower levels, usually below 0.05 $\mu g \cdot L^{-1}$. The main pathways of water contamination by antibiotic residues include direct emissions from pharmaceutical manufacturing facilities, the excretion of metabolized drugs by humans and animals, effluents from aquaculture operations, and improper disposal of unused or expired pharmaceuticals (Gałązka *et al.* 2023; Pereira *et al.* 2023; Oad *et al.* 2023).

Pharmaceutical pollutants must be removed from wastewater before being discharged into the environment; however, due to design limitations, conventional wastewater treatment plants often struggle to eliminate these residues (Moreira *et al.* 2022; Sigonya *et al.* 2023; Oad *et al.* 2023). As a result, over 90% of antibiotic substances persist, leading to their accumulation in domestic and urban wastewater (Becze *et al.* 2022; Oad *et al.* 2023), which poses a significant threat to both aquatic and terrestrial fauna and flora (Ripanda *et al.* 2021; Oad *et al.* 2023).

Indeed, when pharmaceuticals and residues enter human and animal bodies through various water sources, they can lead to adverse effects such as drug resistance and metabolic disturbances (Fallah *et al.* 2021). Additionally, these substances can be transferred through the food chain, impacting non-aquatic animals and humans who consume contaminated fish or other seafood (Fehrenbach *et al.* 2022; Nikoo *et al.* 2023). Therefore, the urgent necessity for eliminating pharmaceutical compounds from wastewater is evident.

To achieve this goal, several conventional treatment techniques were tested, including coagulation-flocculation, adsorption on activated carbon, and biological processes (De Melo Franco Domingos *et al.* 2023; Samir *et al.* 2023; Suleiman *et al.* 2023). While these methods demonstrate effective decontamination, they also generate secondary non-recoverable waste and necessitate further treatment. Additionally, recalcitrant pollutants are not degraded; instead, they are merely transferred from one medium to another (Mansour *et al.* 2021; Fang *et al.* 2023).

Advanced oxidation processes (AOPs), have emerged as a promising solution for the removal of refractory organic compounds from wastewater (Jiad and Abbar 2023). The effectiveness of these technologies relies on the in-situ generation of powerful oxidizing agents, specifically hydroxyl radicals (•OH). AOPs encompass a wide range of established methods, including the Fenton process, Fenton-like processes, high-pH ozonation, wet air oxidation, and photocatalysis whether homogeneous or heterogeneous. Additionally, AOPs cover more complex processes such as peroxide/ozone coupling and ultrasound, as well as advanced electrochemical techniques, notably anodic oxidation and electro-Fenton (Oturan and Aaron 2014; Akpotu *et al.* 2019; Liu *et al.* 2018; Rashmishree *et al.* 2023; Gasmi *et al.* 2023; Mansour *et al.* 2015a; Ljubas *et al.* 2023).

As an indirect oxidation technique, electro-Fenton utilizes the Fenton reaction to generate hydroxyl radicals. A notable aspect of this process is the electrochemical production of both hydrogen peroxide (H_2O_2) and ferrous

ions (Fe^{2+}) during the reaction (Mansour *et al.* 2014; Puga *et al.* 2021; Mahmoudi *et al.* 2022; Mansour *et al.* 2024a). The supplied oxygen is reduced at the cathode to form H_2O_2, which then reacts with the introduced Fe^{2+} ions in acidic conditions, resulting in the formation of hydroxyl radicals (•OH) (Mansour *et al.* 2012; Mansour *et al.* 2015b; Chi *et al.* 2023). Due to its high oxidation potential, •OH can rapidly hydroxylate or dehydrate nearly all organic pollutants, leading to the production of inorganic ions, CO_2 and H_2O (Oturan 2021; García-Espinoza *et al.* 2021; Jiad and Abbar 2023).

Sulfamethazine (SMT) is a widely used sulfonamide antibiotic in veterinary medicine for treating bacterial infections in animals. However, it poses potential threats to human health and aquatic ecosystems. Even at low environmental concentrations (<1 $mg{\cdot}L^{-1}$), frequent use of SMT can lead to the development of antibiotic resistance in bacteria (Mansour *et al.* 2015b; Raj *et al.* 2024). The persistent presence of SMT residues in treated animals, groundwater, surface water, and sediment raises serious concerns. This persistence enhances the potential for bioaccumulation throughout the food chain, ultimately threatening human health (Lin and Huang 2024; Raj *et al.* 2024).

An authoritative critical review by Brillas (Brillas 2025) assessed the performance of advanced oxidation processes for the removal of sulfamethazine across various environmental matrices, including agricultural runoff and wastewater effluents. The evaluation compared Fenton, anodic oxidation, and electro-Fenton systems, with an emphasis on mineralization yields, the generation of reactive oxygen species, and the formation of intermediate by-product. To ensure the environmental safety of the treated effluents, the study also tracked the changes in solution toxicity during the oxidation process. Importantly, this analysis underscores that implementing these technologies on a large-scale still necessitates significant engineering and catalytic advancements.

Given these operational barriers, previous studies - including our own (Mansour *et al.* 2014)- have applied electro-Fenton as a pre-treatment to convert sulfamethazine (SMT) into more biodegradable intermediates for subsequent biological processing. The current study advances electro-Fenton into an independent mineralization system. To this end, this work aims to achieve two main objectives: first, to determine the optimal operational conditions for the mineralization of synthetic sulfamethazine effluent using the electro-Fenton process, employing a Doehlert design combined with Response Surface Methodology (RSM). A quadratic model was applied within the Doehlert experimental design to simultaneously examine several parameters at varying levels. This strategy reduces the number of required experiments while maintaining the quality of results, thereby providing an effective method for variable optimization (El Faroudi *et al.* 2023). This approach allows the simultaneous examination of several factors and offers insights into individual impacts as well as their interactions, representing a significant advancement over the traditional univariate strategy (El Faroudi *et al.* 2023). To achieve this goal, the mineralization rate of sulfamethazine was evaluated by monitoring the decrease in total organic carbon (TOC) during electrolysis. The second objective is to quantify and monitor the evolution of concentrations of aliphatic acids and ionic species generated during remediation. In summary, this project aims to enhance sustainable wastewater treatment methods, thereby reducing the discharge of organic pollutants into ecosystems.

2. Materials and Methods

2.1. *Chemicals*

Sulfamethazine (99% purity) was purchased from Sigma Aldrich (Saint-Quentin-Fallavier, France). $FeSO_4.7H_2O$ (99% purity) and Na_2SO_4 (99% purity), used as reactant and electrolyte support respectively, were provided by Acros Organics (Thermo Fisher Scientific, Illkirch, France). The pH of treated solutions was adjusted using analytical grade sulfuric acid (H_2SO_4) obtained from Acros Organics. All solutions were prepared using ultrapure water. Sigma Aldrich and Acros Organics supplied all analytical grade chemicals.

2.2. *Analytical determinations*

2.2.1. Total Organic Carbon (TOC) measurements

To quantify the mineralization of the pollutant, total organic carbon (TOC) analysis was exclusively utilized. Compared to standard chemical oxygen demand (COD) measurements, which are susceptible to overestimation due to interferences from residual hydrogen peroxide and other inorganic species common in advanced oxidation processes, TOC provides a fundamentally more accurate and direct assessment of organic carbon removal (Al-Qodah *et al.* 2024; Al-Qodah *et al.* 2025).

Prior to analysis, samples from the electro-Fenton treatment were filtered through 0.40 µm GF filters (Sartorius Stedim Minisart, Göttingen, Germany). Their TOC content was then determined using a TOC-VCPH/CPN analyzer (Shimadzu Corporation, Kyoto, Japan). In this process, the organic matter is oxidized to form CO_2, which is subsequently detected by a non-dispersive infrared (NDIR) sensor. The standard NPOC (Non-Purgeable Organic Carbon) method was employed, and all measurements were performed in triplicate to ensure reproducibility (Mansour *et al.* 2015b).

2.2.2. Ion chromatography

The by-products of sulfamethazine mineralization, specifically carboxylic acids, nitrate, and sulfate ions, were analyzed by ion chromatography using a Dionex DX120 system equipped with conductivity detection. The analysis process was carried out as follows: the separation was performed using a Dionex AS19 analytical column (4 × 250 mm), equipped with a Dionex AG19 guard column (4 × 50 mm), and an ASRS suppressor; and a KOH gradient generated by a Dionex ECG-KOH EluGen II cartridge, flowing at a rate of 1 $mL{\cdot}min^{-1}$, was used as mobile phase. The elution profile was programmed as follows: an initial isocratic hold at 10 mM (0-10 min), followed by a linear

gradient from 10 to 45 mM (10-25 min), and concluding with an isocratic step at 45 mM (25-35 min). Data acquisition and system control were performed using Chromeleon software.

2.2.3. Ammonium quantification

The ammonium (NH_4^+) concentration was determined using Nanocolor® tests Ammonium 3 (Ref 985 003) from Macherey-Nagel (Germany). All measurements were made using a photometer type Nanocolor®.

2.3. *Experimental Procedure*

The sulfamethazine mineralization was performed via the electro-Fenton process in a 1-liter undivided glass cell fitted with two electrodes (**Figure 1**). The cathode was a carbon felt electrode (Le Carbone Lorraine RVG 4000, Mersen, Paris, France), characterized by dimensions of 260 mm × 80 mm, a specific area of 0.7 $m^2\ g^{-1}$, a thickness of 12 mm, a density of 0.088 g cm^{-3}, and a 99.9% carbon yield, and was placed along the inner wall of the cell. A cylindrical platinum anode (50 mm × 20 mm) was placed at the center of the electrochemical reactor to ensure an even potential distribution. A peristaltic pump was used to continuously circulate the electrolyte solution at a rate of 2 L min^{-1}. Na_2SO_4 was added to the medium in order to keep the ionic strength at 0.05 M. To reach oxygen saturation, compressed air was bubbled through the solution for ten minutes at a flow rate of 450 $cm^3\ min^{-1}$. Sulfuric acid (H_2SO_4) was used to adjust the pH of sulfamethazine solutions to 3. Finally, just prior to the treatment, a catalytic amount of $FeSO_4.7H_2O$ was added to the cell. In order to maintain a constant current, electrolysis was carried out under galvanostatic control using a DC power supply (Model AX 322, Metrix, Annecy, France)

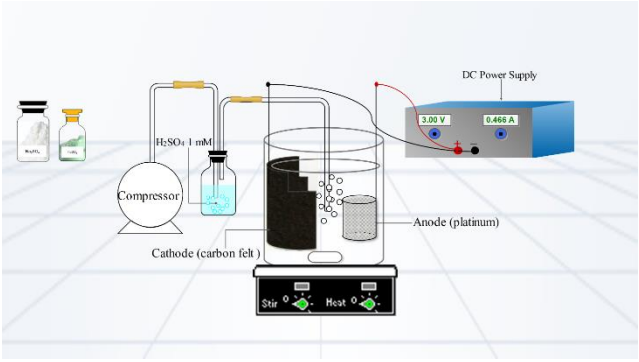


Figure 1. Schematic diagram of the electro-Fenton apparatus employed for the mineralization of sulfamethazine.

2.4. *Doehlert experimental design*

In order to maximize the mineralization of sulfamethazine, a Doehlert design was implemented. Three important experimental parameters were studied, namely: current intensity (U_1), electrolysis time (U_2), and initial concentration of Fe^{2+} (U_3). The response variable (Y) was defined as the TOC removal efficiency.

The formula $N = k^2 + k + 1$ (where k is the number of parameters) was used to construct the experimental set and determine the number of trials. Accordingly, for k=3, the matrix consisted of 13 experiments, uniformly distributed throughout the coded experimental region. The measurement at the central point was performed in triplicate (experiments 13 to 15), and included in the design to estimate the experimental error. Natural variables (U_i) were converted to coded variables (X_i) according to equation 1 (Hammami *et al.* 2009):

$$X_i = \left[\frac{U_i - U_{i(0)}}{\Delta U_i}\right]\alpha \quad (1)$$

In this equation, $U_{i\ (0)}$ is the central value of the experimental domain and ΔU_i is the variation step. The parameter α represents the maximum coded value for each variable, set at 1 for X_1, 0.866 for X_2, and 0.816 for X_3.

$$U_{i(0)} = \frac{\textit{upper limit of } U_i + \textit{lower limit of } U_i}{2} \quad (2)$$

$$\Delta U_i = \frac{\textit{upper limit of } U_i - \textit{lower limit of } U_i}{2} \quad (3)$$

The experimental domains for the Doehlert design were established based on preliminary trials (data not shown): $0.1 < U_1$ (A) < 0.5; $2 < U_2$ (h) < 18; and $0.1 < U_3$ (mM) < 0.9).

The experimental response was fitted to a quadratic polynomial equation based on the Doehlert matrix.

$$Y = b_0 + b_1X_1 + b_2X_2 + b_3X_3 + b_{11}X_1^2 + b_{22}X_2^2 + b_{33}X_3^2 + b_{12}X_1X_2 + b_{13}X_1X_3 + b_{23}X_2X_3 \quad (4)$$

In this equation, Y represents the experimental response and b_0 is the model intercept.

b_i, b_{ii}, and b_{ij} are the estimated regression coefficients corresponding to the linear, quadratic, and interaction terms.

The coefficients were determined using the least squares method according to the equation (5):

$$B = (X^T X)^{-1} X^T Y \quad (5)$$

B is the vector of estimated coefficients, X is the design matrix (where X^T is its transpose), and Y represents the measured response vector.

The suitability and statistical significance of the model were verified using the analysis of variance (ANOVA). The two-dimensional isoresponse curves and their corresponding three-dimensional response surfaces were used to illustrate the relationship between the experimental variables and the response. NEMRODW software was employed for all data processing (Mathieu *et al.* 2000).

3. Results and Discussion

3.1. *Optimization of process conditions for the sulfamethazine mineralization*

Several parameters, such as the intensity of applied current, the electrolysis time, and the initial concentration of Fe^{2+}, influence the efficiency of the electro-Fenton process. Therefore, a Doehlert matrix was utilized to identify the optimal conditions that yield the highest mineralization rate. **Table 1** displays the experimental design

Table 1. Doehlert matrix experiments and experimental results.

Experiment number	Coded variables			Real variables			Results
	X_1	X_2	X_3	Current intensity:	Electrolysis time:	Fe^{2+} concentration:	Y (%)
				U_1 (A)	U_2 (h)	U_3 (mM)	
1	1	0	0	0.5	10	0.5	79.1
2	-1	0	0	0.1	10	0.5	57.7
3	$\frac{1}{2}$	$\frac{\sqrt{3}}{2}$	0	0.4	18	0.5	81.5
4	$-\frac{1}{2}$	$-\frac{\sqrt{3}}{2}$	0	0.2	2	0.5	35.9
5	$\frac{1}{2}$	$-\frac{\sqrt{3}}{2}$	0	0.4	2	0.5	43.3
6	$-\frac{1}{2}$	$\frac{\sqrt{3}}{2}$	0	0.2	18	0.5	73.8
7	$\frac{1}{2}$	$\frac{\sqrt{3}}{6}$	$\frac{\sqrt{6}}{3}$	0.4	13	0.9	74.5
8	$-\frac{1}{2}$	$-\frac{\sqrt{3}}{6}$	$-\frac{\sqrt{6}}{3}$	0.2	7	0.1	48.2
9	$\frac{1}{2}$	$-\frac{\sqrt{3}}{6}$	$-\frac{\sqrt{6}}{3}$	0.4	7	0.1	61.5
10	0	$-\frac{\sqrt{3}}{3}$	$-\frac{\sqrt{6}}{3}$	0.3	15	0.1	70.2
11	$-\frac{1}{2}$	$\frac{\sqrt{3}}{6}$	$\frac{\sqrt{6}}{3}$	0.2	13	0.9	65.1
12	0	$-\frac{\sqrt{3}}{3}$	$\frac{\sqrt{6}}{3}$	0.3	5	0.9	54.7
13	0	0	0	0.3	10	0.5	69.0
14	0	0	0	0.3	10	0.5	71.5
15	0	0	0	0.3	10	0.5	74.0

The model equation presented in equation (6) was derived by calculating the coefficients of the polynomial regression based on the experimental results shown in **Table 1**.

$$Y = 71.5 + 10.1\ X_1 + 20.9\ X_2 + 2.9\ X_3 - 3.1\ X_1^2 - 16.1\ X_2^2 - 8.9\ X_3^2 + 0.2\ X_1X_2 - 2.5\ X_1X_3 - 4.8\ X_2X_3 \quad (6)$$

Table 2. Result of variance analysis for the removal of TOC.

Source of variation	Sum of squares	Degrees of freedom	Mean square	*F*-ratio	*p*-value
Regression	2525.88	9	280.65	39.27	<0.001
Residual	35.74	5	7.15		
Lack of Fit	23.24	3	7.75	1.24	0.474
Pure Error	12.50	2	6.25		
Total	2561.62	14			

Note: $R^2 = 0.986$; $R^2_{adj} = 0.961$.

Analysis of variance (ANOVA) was conducted to evaluate the quadratic model (equation 6). As indicated in **Table 2**, the regression is significant ($p < 0.001$), while the lack-of-fit is non-significant ($p = 0.474$), suggesting that the model fits the experimental data adequately. The determination coefficients ($R^2 = 0.986$; $R^2_{adj} = 0.961$) indicate that the model explains 98.6% of the response variation. Diagnostic plots (**Figure 2**) reinforce the statistical assumptions. The normal probability plot (**Figure 2a**) confirms that the residuals follow a normal distribution. The Studentized residuals versus predicted values (**Figure 2b**) display a random, homogeneous dispersion within the ± 2 interval, demonstrating the absence of systematic error during the experiments.

The isoresponse curves and 3D response surfaces illustrating the variation of TOC removal are presented in

Figure 4. These results clearly demonstrate a positive correlation between current intensity and TOC removal efficiency. Under constant conditions of [Fe^{2+}] = 0.5 mM and an electrolysis time of 10 h, increasing the current intensity from 0.1 A to 0.5 A resulted in an increase of the TOC removal rate from 58.4% to 78.5%. This indicates that enhancing the electrical power supplied to the reactor improves treatment efficiency (**Figure 4a-b**).

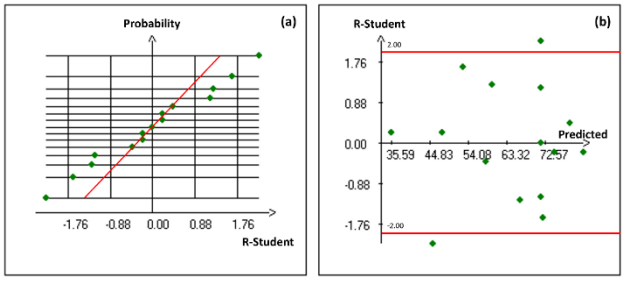


Figure 2. Diagnostic plots for the response surface model of sulfamethazine mineralization: (a) normal probability plot of residuals and (b) residuals versus fitted values.

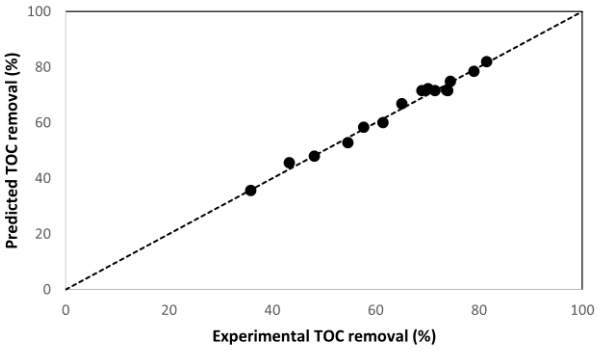


Figure 3. Parity plot of the experimental versus predicted values for TOC removal efficiency.

The observed improvement in TOC removal rates can be attributed to the efficient regeneration of the Fe^{2+} ions (equation (7)) and the continuous production of hydrogen peroxide H_2O_2 at the cathode (equation (8)). This process promotes the production of hydroxyl radicals (equation (9)), thereby enhancing treatment efficiency (Atmaca 2009; Mansour *et al.* 2015a; Mansour *et al.* 2026)

$$Fe^{3+} + e^- \rightarrow Fe^{2+} \quad (7)$$

$$O_2 + 2e^- + 2H^+ \rightarrow H_2O_2 \quad (8)$$

$$Fe^{2+} + H_2O_2 \rightarrow OH^- + Fe^{3+} + {}^{\bullet}OH \quad (9)$$

$$2H_2O \rightarrow O_2 + 4H^+ + 4e^- \quad (10)$$

$$2H_2O + 2e^- \rightarrow H_2 + 2OH^- \quad (11)$$

Within the context of electrochemical advanced oxidation, it is essential to clearly distinguish between primary degradation and ultimate mineralization. Primary degradation refers to the rapid initial attack by hydroxyl radicals, which leads to the cleavage of the sulfamethazine (SMT) aromatic ring and the swift disappearance of the parent molecule. In contrast, ultimate mineralization signifies the complete electrochemical conversion of the resulting organic matrix into CO_2, H_2O, and inorganic heteroatoms. As assessed in this study, mineralization is quantitatively measured by total organic carbon (TOC) removal. This ultimate conversion occurs at a slower kinetic rate than primary degradation, primarily due to the formation and transient accumulation of refractory short-chain aliphatic intermediates, which necessitate prolonged electrolysis to achieve complete oxidation.

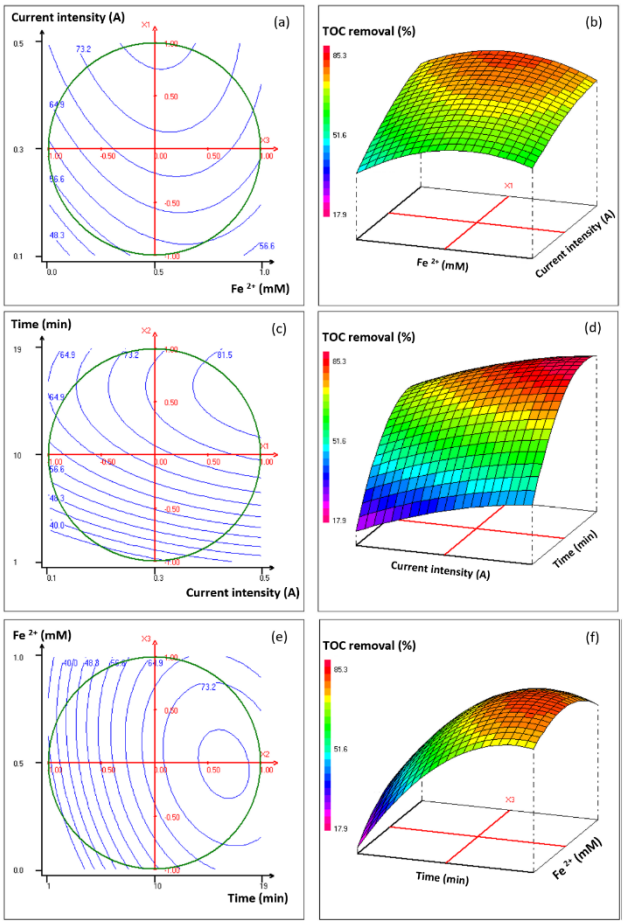


Figure 4. (a) TOC removal efficiency contours versus the intensity of current (A) and the Fe^{2+} concentration (mM); (b) The 3D surface plot that corresponds; (c) TOC removal efficiency contours versus the time of reaction (h) and the intensity of current (A); (d) The 3D surface plot that corresponds; (e) TOC removal efficiency contours versus the Fe^{2+} concentration (mM) and the time of reaction (h); (f) The 3D surface plot that corresponds. Data collected through the matrix of Doehlert (**Table 1**). Operating conditions: [SMT] = 0.2 mM, pH=3, [Na_2SO_4] = 50 mM, V = 1 L.

Furthermore, the graphic analysis of **Figures 4c and 4d** shows that the TOC removal efficiency increased with longer electrolysis times. Specifically, for [Fe^{2+}] = 0.5 mM and I = 0.3 A, extending the treatment duration from 2 to 16 hours raised the TOC removal rate from 34.8% to 78.3%. However, increasing the electrolysis time from 16 to 18 hours resulted in a decline in the mineralization rate, dropping from 78.3% to 76.8%. This decrease is attributed to the occurrence of parasitic reactions and the scavenging of hydroxyl radicals (•OH) by stable by-products that accumulate during prolonged treatment periods. The optimum current intensity was determined at the upper limit of the experimental domain (0.5 A). Higher currents were excluded to avoid excessive Joule heating, anodic

oxygen evolution (equation (10)), and a subsequent decrease in faradaic efficiency.

On the other hand, when the initial concentration of ferrous ions ([Fe^{2+}]) was increased from 0.1 to 0.5 mM, the TOC removal rate improved from 59.7% to 71.6%. The best results were achieved within a concentration range of 0.4 to 0.6 mM (**Figure 4e and f**). This increase in efficiency can be attributed to the enhanced production of $^{\bullet}OH$, which is favored by the higher availability of Fe^{2+} ions in the medium (Panizza and Cerisola 2009). However, increasing the initial Fe^{2+} ions concentration from 0.6 to 0.9 mM led to a decrease in mineralization rate from 71.4% to 65.6%. This reduction occurred because the excess ferrous ions acted as scavengers for $^{\bullet}OH$ (equation (12)), thereby decreasing the concentration of these radicals and reducing the oxidizing capacity of the system (Panizza and Cerisola 2009; Brillas *et al.* 2009).

$$Fe^{2+} + {}^{\bullet}OH \rightarrow Fe^{3+} + OH^{-} \quad (12)$$

A confirmatory electrolysis trial was conducted under the established optimal conditions ([Fe^{2+}] = 0.5 mM, t = 16 h, I = 0.5 A). The quadratic model predicted a TOC removal efficiency of 85.3% with a 95% confidence interval of [82.0% - 88.6%]. As shown by the kinetic study (**Figure 5**), the empirical measurement yielded a 90.0% reduction with a standard deviation of $\pm 3.0\%$, establishing an experimental range of [87.0% - 93.0%]. The relative error between the predicted and experimental values is 5.5%. The overlap between the predicted and experimental intervals indicates statistical agreement.

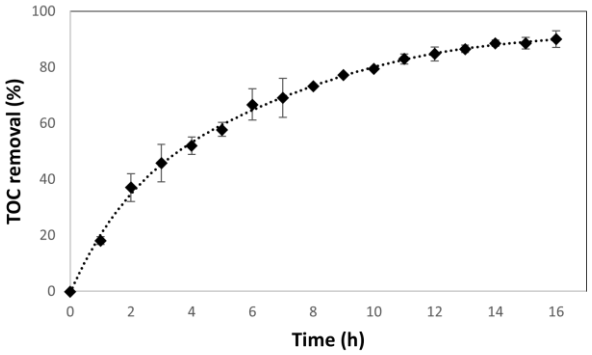


Figure 5. Time evolution of TOC removal rate (%). Operating conditions: [SMT] = 0.2 mM, pH=3, [Na_2SO_4] = 50 mM, [Fe^{2+}] = 0.5 mM, V = 1L, I = 0.5 A.

Figure 5 illustrates a rapid initial increase in the TOC removal efficiency, reaching 77.2% within the first 9 hours of electrolysis. Following this initial phase, the rate of mineralization significantly slows down. Nevertheless, the TOC level continues to decrease slightly over time, leading to a 90% reduction by the end of the treatment. This behavior occurs because the electro-Fenton degradation of sulfamethazine generates aromatic intermediates, which are subsequently oxidized by hydroxyl radicals into short-chain carboxylic acids through ring cleavage (Mansour *et al.* 2015a). Aromatic compounds, due to their delocalized electrons, can stabilize the intermediates formed during reactions with •OH radicals (Haidar *et al.* 2013; Mansour *et al.* 2014). According to Haidar *et al.* (Haidar *et al.* 2013), hydroxyl radicals preferentially attack aromatic intermediates rather than carboxylic acids, which show significant resistance to oxidation by •OH radicals. Additionally,, this behavior may arise from the formation of Fe (III) complexes with carboxylic acids during the process (Mansour *et al.* 2024b). The stability of these species and their limited reactivity toward hydroxyl radicals lead to a decrease in mineralization efficiency compared to the initial treatment phase.

3.2. *Mineralization monitoring: Evolution of terminal by-products*

In order to characterize the overall electro-Fenton oxidation process, the identification of the main initial aromatic intermediates has been previously conducted by LC-MS/MS analysis (Mansour *et al.* 2014). Concomitantly to these initial fragmentation steps, the current analytical monitoring strictly focuses on the terminal mineralization phase. Generated short-chain carboxylic acids and released inorganic ions were tracked to quantitatively confirm the mineralization of SMT.

3.2.1. Short-chain carboxylic acids' evolution

Successive attacks by •OH radicals progressively destabilize aromatic compounds, ultimately leading to the breakdown of the aromatic ring structure. This process results in the production of hydrocarbons containing carboxyl functional groups, as well as aldehydes, ketones or alcohols. Due to the highly oxidizing nature of the medium, it facilitates the sequential conversion of alcohols into aldehydes and, subsequently, into carboxylic acids (Chou *et al.* 1999).

Glyoxylic, succinic, and oxalic acids were identified as oxidation products derived from the aromatic intermediates of sulfamethazine during the electro-Fenton treatment. The evolution of their concentration throughout electrolysis was monitored, and the resulting data are illustrated in **Figure 6**.

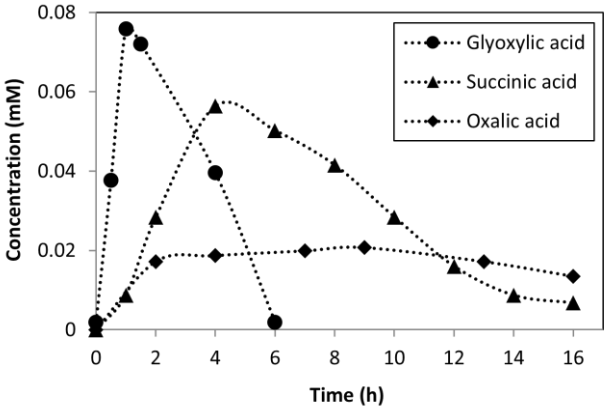


Figure 6. Carboxylic acids concentration versus reaction time. Operating conditions: [SMT] = 0.2 mM, pH=3, [Na_2SO_4] = 50 mM, [Fe^{2+}] = 0.5 mM, V = 1L, I = 0.5 A.

The obtained results indicate that the carboxylic acids detected during the SMT treatment are formed at the beginning of electrolysis. A rapid accumulation of glyoxylic acid was observed, reaching a maximum concentration of 0.076 mM after 1 hour of reaction time, after which it was degraded until total disappearance. In addition, the concentration of succinic acid increased during the

treatment, attaining a maximum concentration of 0.056 mM after 4 hours, before subsequently decreasing.

On the other hand, oxalic acid accumulated in small amount, peaking at 0.02 mM, and its concentration decreased slightly after 9 hours of electrolysis. Notably, these last two acids are very recalcitrant. Indeed, even after 16 hours electrolysis, small amounts of oxalic and succinic acid persisted in the SMT solutions. This behavior can be attributed first to their low reactivity towards hydroxyl radicals, and second to the formation of stable ferric-carboxylate complexes, which are difficult to oxidize by hydroxyl radicals (Özcan *et al.* 2013; El-Ghenymy *et al.* 2013).

3.2.2. Inorganic ions' evolution

The heteroatoms present in the SMT molecule were formed during the mineralization process as inorganic ions. The presence of sulfate, nitrate, and ammonium ions, resulting from the sulfur and nitrogen atoms in the SMT structure, has been previously verified (Mansour *et al.* 2014). Furthermore, no traces of nitrite ions were detected. To examine the evolution of inorganic ions during the mineralization of SMT, quantitative analysis of these ions was conducted, and their concentration changes during electrolysis were analyzed. The obtained data are illustrated in **Figure 7**.

During the electro-Fenton process, the sulfur and nitrogen heteroatoms within the SMT structure were released as inorganic ions. **Figure 6** presents the kinetic evolution of these species. The formation of sulfate was rapid during the first hour, attributed to the high reactivity of •OH radicals towards the –SO_2– group (Hammami *et al.* 2007). Following this initial phase, the rate of sulfate formation gradually decreased. Ammonium ions were produced immediately upon the onset of electrolysis. Nitrate formation exhibited a 2-hour induction period before increasing and exceeding the NH_4^+ concentration. This observation suggests the anodic oxidation of NH_4^+ to NO_3^- on the platinum electrode (Özcan *et al.* 2013).

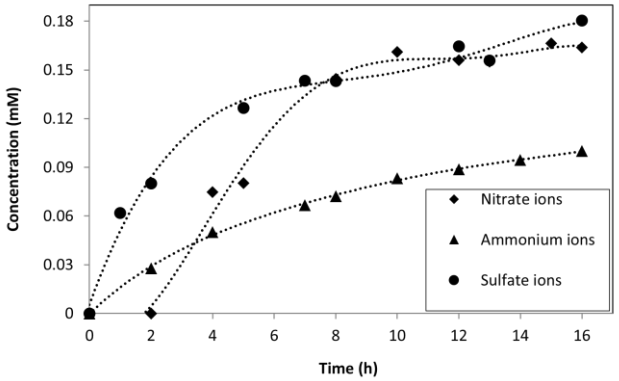


Figure 7. Inorganic ions concentration versus reaction time. Operating conditions: [SMT] = 0.2 mM, pH=3, [Na_2SO_4] = 50 mM, [Fe^{2+}] = 0.5 mM, *V* = 1L, *I* = 0.5 A.

Table 3. Systematic mass-balance of inorganic ions at optimal conditions.

Element	Theoretical content (mM)	Final recovered species (mM)	Recovery (%)
Sulfur (S)	0.20	SO_4^{2-} : 0.18	90%
Nitrogen (N)	0.80	NH_4^+: 0.10	
NO_3^-: 0.16	33%		

Table 3 presents the mass balance at 16 hours. The recovery of sulfate reached 90.0% of the theoretical content. The final concentrations of NO_3^- and NH_4^+ were measured at 0.16 mM and 0.10 mM, respectively. However, the nitrogen mass balance reflects only 33% of the theoretical value, indicating a deficit.. This deficit may be attributed to volatile species (N_2, N_xO_y) or unidentified refractory organic nitrogen compounds associated with the residual TOC, though this remains a hypothesis. Consequently, the mechanistic interpretation of nitrogen cleavage is partial.

3.3. *Cost analysis and comparative evaluation*

The total operating cost per gram of TOC removed (OC_{TOC}) for the mineralization of SMT by the electro-Fenton process includes the costs of consumed electrical energy, chemicals, labor, and maintenance (Suhan *et al.* 2020). To determine this cost, the consumption of energy per gram of TOC removed (ENC_{TOC}) and the consumption of chemicals per gram of TOC removed (CHC_{TOC}) for 1 m^3 of pharmaceutical wastewater were calculated using to the following equations (Mansour *et al.* 2014; Suhan *et al.* 2020).

$$ENC_{TOC}\left(\text{kWh}\cdot\text{g}^{-1}\ \text{TOC}\right)=\frac{U\times I\times t\times 10^{-3}}{V\times\Delta\left(\text{TOC}\right)_{exp}} \quad (13)$$

Where, *U*: the applied cell voltage, empirically measured at a constant 3.5 V, *I*: the intensity of current (A), *t*: the electrolysis time (h), *V*: the wastewater volume (m^3), and $\Delta(TOC)_{exp}$: the experimental decay of total organic carbon ($g\cdot m^{-3}$).

$$CHC_{TOC}\left(\text{kg}\cdot\text{g}^{-1}\ \text{TOC}\right)=\frac{\rho_i}{\Delta\left(\text{TOC}\right)_{exp}} \quad (14)$$

The obtained results indicate that under the optimal conditions (section 3.1), the electro-Fenton process required an electrical energy consumption of 1.2 $kWh\cdot g^{-1}$ TOC. The consumptions of ferrous sulfate and sodium sulfate were 6.1×10^{-3} $kg\cdot g^{-1}$ TOC and 3.1×10^{-1} $kg\cdot g^{-1}$ TOC, respectively.

The total operating cost per gram of TOC removed (OC_{TOC}) was calculated using the following equation (Bel Hadj Hmida *et al.* 2010; Suhan *et al.* 2020)

$$OC_{TOC}=a\times ENC_{TOC}+b\times CHC_{TOC}\ (Fe^{2+})+c\times CHC_{TOC}\ (Na_2SO_4)+Cost_{other} \quad (15)$$

Where a is the electricity cost (0.05 USD/kWh), b is the ferrous sulfate cost (0.25 USD/kg), and c is the sodium sulfate cost (0.15 USD/kg), and Cost $_{other}$ represents the estimated maintenance and labor costs (6.3×10^{-5}USD) (Suhan *et al.* 2020). Based on these industrial bulk prices, the operating cost is 0.108 USD·g^{-1} TOC.

Scale-up to 1 m^3 assumes direct linear volumetric extrapolation from the 1 L bench-reactor. This preliminary estimation excludes industrial parameters such as capital expenditure (CAPEX) and sludge management. Economic benchmarking evaluates the specific cost (0.108 USD·g^{-1} TOC) against literature values for the advanced oxidation of recalcitrant matrices (0.063 - 0.905 USD·g^{-1} TOC for anodic oxidation (Can *et al.* 2021)). This calculation confirms the published electro-Fenton benchmark (0.117 USD·g^{-1} TOC) and yields a lower operational cost compared to photo-Fenton (0.174 USD·g^{-1} TOC) and ozonation (1.04 USD·g^{-1} TOC) (Mousset *et al.* 2021).

Table 4. Comparative performance of various electrochemical advanced oxidation processes for sulfamethazine (SMT) mineralization.

Process	Operating Conditions	Mineralization (TOC Removal (%))	Energy Consumption	Reference
Homogeneous electro-Fenton (BDD | GF)	[SMT] = 0.2 mM, [Fe^{2+}] = 0.2 mM, [Na_2SO_4] = 50 mM, pH 3.0, t = 480 min, j = 20.83 mA·cm^{-2}.	90	2.8 kWh·g^{-1} TOC	(Sopaj *et al.* 2016)
Dual-cathode electro-Fenton (DSA | NAD and MCF)	[SMT] = 100 mg·L^{-1}, [Fe^{3+}] = 0.5 mM, [Na_2SO_4] = 50 mM, pH 7.0, t = 60 min,j_{NAD} = 40 mA·cm^{-2}, j_{MCF} = 10 mA·cm^{-2}.	47	0.141 kWh·g^{-1} TOC	(Zhang *et al.* 2022)
Anodic Oxidation(Sm-Ti_4O_7 | Ti)	[SMT] = 10 mg·L^{-1}, [Na_2SO_4] = 50 mM, pH 5.0, t = 60 min, j = 20 mA·cm^{-2}.	80	0.035 kWh·g^{-1} COD*	(Tao *et al.* 2025)
Heterogeneous electro-Fenton (Pt | CF-Fe)	[SMT] = 30 mg·L^{-1}, [Na_2SO_4] = 50 mM, pH 5.0, t = 120 min, I = 50 mA.	70	0.0012 kWh·g^{-1} COD*	(Aissani *et al.* 2023)
Homogeneous electro-Fenton (Pt | CF)	[SMT] = 0.2 mM, [Fe^{2+}] = 0.5 mM, [Na_2SO_4] = 50 mM, pH 5.0, t = 16h, I = 0.5 A.	90	1.2 kWh·g^{-1} TOC	This Study

BDD: Boron-Doped Diamond. GF: Graphite felt. CF: Carbon felt. DSA: Dimensionally Stable Anode. NAD: Natural Air-Diffusion. MCF: Modified Carbon Felt.

** Note: Energy consumption values originally reported in kWh/kg COD were mathematically converted to kWh/g COD to provide a uniform scale comparison with the kWh/g TOC values obtained in this study*

Table 4 benchmarks the optimized electro-Fenton process against current literature. Achieving high mineralization of recalcitrant organic pollutants requires a compromise between kinetic efficiency and energy consumption. Certain advanced oxidation methods report minimal energy requirements, limiting TOC removal to approximately 47% (Zhang *et al.* 2022). Conventional homogeneous electro-Fenton reactors achieve a 90% mineralization yield, requiring an energy input of 2.8 kWh·g^{-1} TOC (Sopaj *et al.* 2016). The Doehlert optimization in this study achieved a 90.0% TOC removal with a restricted energy demand of 1.2 kWh·g^{-1} TOC.

3.4. *Process stability and operational limitations*

Electrode conductivity remains stable; however, sustained electrocatalytic performance is impeded by surface passivation and pH fluctuations. Platinum (Pt) anodes undergo rapid deactivation. During SMT mineralization, organic intermediates electropolymerize and chemisorb onto the Pt surface, forming a passivating film that deactivates electrochemically active sites. Unbalanced water electrolysis independently drives bulk pH drift. Exceeding a pH limit of 3.0 induces the precipitation of the homogeneous iron catalyst into inactive ferric hydroxide species. Preserving faradaic efficiency dictates active operational control. Essential interventions include periodic polarity reversal to electrochemically desorb the organic layer and in-line acid titration to stabilize the required acidic medium.

Beyond the immediate constraints of the laboratory, the direct application of these findings to industrial wastewater treatment is limited by specific operational boundaries. The use of a synthetic solution prevents the assessment of matrix effects, particularly the radical scavenging interference from background inorganic species typical of real effluents. Operationally, the process requires adjustments to acidic conditions (pH 3) and prolonged electrolysis times. Furthermore, scaling up the process necessitates careful evaluation of capital expenditures (CAPEX), largely due to the high costs and rapid passivation associated with platinum anodes. Finally, although total organic carbon (TOC) removal indicates chemical mineralization, it does not automatically ensure environmental safety; thorough ecotoxicity assessments are essential before any real-world implementation.

4. Conclusions

The electrochemical advanced oxidation of sulfamethazine was effectively modeled and optimized using a Doehlert experimental design. By adjusting current intensity, reaction time, and Fe^{2+} dosage, a mineralization efficiency of 90% was achieved after 16 hours. The statistical analysis confirms that the obtained quadratic polynomial model

accurately describes the experimental data. Furthermore, the energy consumption for the mineralization of SMT by the electro-Fenton process was evaluated at 1.2 $kWh \cdot g^{-1}$ TOC. The quantification of short-chain carboxylic acids indicated their accumulation and subsequent slow degradation, demonstrating their resistance to hydroxyl radical attack. Similarly, the monitoring of released inorganic ions confirmed the high but incomplete oxidation of the parent molecule.

This study establishes optimal batch conditions for the electro-Fenton process. Industrial scaling up necessitates a shift to continuous-flow electrolysis to maintain high mineralization rates while ensuring energy efficiency. This operational approach requires automated in-line pH control, steady oxygen sparging, and the integration of 3D heterogeneous reactors to eliminate the need for continuous iron dosing. Beyond reactor design, the presence of degradation intermediates indicates that achieving chemical efficiency does not automatically ensure environmental safety. Future research should prioritize standardized ecotoxicity assays and long-term evaluations of electrode stability before any real-world applications.

Acknowledgments

The authors express their sincere thanks to the University of Hail, Kingdom of Saudi Arabia for financing this study. Thanks go also to the Chemistry Department of College of Sciences at Hail University for their valuable assistance in providing with the required information.

Funding

This research has been funded by Scientific Research Deanship at University of Hail – Saudi Arabia through project number RG–21 171.

Data Availability Statement

The data that support the findings of this study are available from the corresponding author upon reasonable request.

Conflicts of Interest

The authors declare that they have no known competing financial interests or personal relationships that could appear to influence the work reported in this paper.

References

Aissani T, Fourcade F, Yahiaoui I, Amrane A, Aissani-Benissad F (2023) Heterogeneous Electro-Fenton Process Using a Cathode of Carbon Felt Impregnated with Iron for the Degradation and Biodegradability Enhancement of Sulfamethazine. Int J Environ Res 17(6):61. https://doi.org/10.1007/s41742-023-00550-w

Akpotu SO, Oseghe EO, Ayanda OS, Skelton AA, Msagati TAM, Ofomaja AE (2019) Photocatalysis and biodegradation of pharmaceuticals in wastewater: effect of abiotic and biotic factors. Clean Techn Environ Policy 21(9):1701–1721. https://doi.org/10.1007/s10098-019-01747-4

Al-Qodah Z, Al-Shannag M, Hudaib B, Bani-Salameh W (2024) Enhancement of dairy wastewater treatment efficiency in batch chemical-assisted solar-powered electrocoagulation-adsorption system. Case Studies in Chemical and Environmental Engineering 9:100760. https://doi.org/10.1016/j.cscee.2024.100760

Al-Qodah Z, Al-Shannag M, Hudaib B, Bani-Salameh W, Shawaqfeh AT, Assirey E (2025) Synergy and enhanced performance of combined continuous treatment processes of pre-chemical coagulation (CC), solar-powered electrocoagulation (SAEC), and post-adsorption for Dairy wastewater. Case Studies in Chemical and Environmental Engineering 11:101183. https://doi.org/10.1016/j.cscee.2025.101183

Atmaca E (2009) Treatment of landfill leachate by using electro-Fenton method. Journal of Hazardous Materials 163(1):109–114. https://doi.org/10.1016/j.jhazmat.2008.06.067

Becze A, Resz M-A, Ilea A, Cadar O (2022) A Validated HPLC Multichannel DAD Method for the Simultaneous Determination of Amoxicillin and Doxycycline in Pharmaceutical Formulations and Wastewater Samples. Applied Sciences 12(19):9789. https://doi.org/10.3390/app12199789

Bel Hadj Hmida ES, Mansour D, Bellakhal N (2010) Treatment of lixiviate from Jebel Chakir-Tunis by electrocoagulation. Desalination and Water Treatment 24(1–3):266–272. https://doi.org/10.5004/dwt.2010.1601

Brillas E (2025) Advances of sulfamethazine removal from aqueous matrices by Fenton, photo-Fenton, and electrochemical advanced oxidation processes. Next Chemical Engineering 1:100008. https://doi.org/10.1016/j.nxcen.2025.100008

Can OT, Tutun MM, Keyikoglu R (2021) Anodic oxidation of bisphenol A by different dimensionally stable electrodes. Water Science and Technology 83(8):1907–1919. https://doi.org/10.2166/wst.2021.092

Chi C, Zhou X, Wang Y, Gao X, Bai J, Guo Y, Ni J (2023) Treatment of coking wastewater using a needle coke electro-Fenton cathode: optimizing of COD, NH4+-N, and TOC removal and characterization of pollutants. Water Science & Technology 88(1):106–122. https://doi.org/10.2166/wst.2023.172

Chou S, Huang Y-H, Lee S-N, Huang G-H, Huang C (1999) Treatment of high strength hexamine-containing wastewater by electro-Fenton method. Water Research 33(3):751–759. https://doi.org/10.1016/S0043-1354(98)00276-0

De Melo Franco Domingos J, De Alencar Neves T, De Sousa Maia DL, Carvalho Siqueira R, Araújo Marques MV, Alves OL, Guimarães JR, Antunes Nolasco M, Rosa AH (2023) Effect of the association of coagulation/flocculation, hydrodynamic cavitation, ozonation and activated carbon in landfill leachate treatment system. Sci Rep 13(1):9502. https://doi.org/10.1038/s41598-023-36662-8

El Faroudi L, El Jemli Y, Zari R, Barakat A, Ismael MK, Abdelouahdi K, Solhy A (2023) Optimization of photocatalytic parameters using Doehlert experimental design to improve the photodegradation of Orange G. Journal of Photochemistry and Photobiology A: Chemistry 445:115012. https://doi.org/10.1016/j.jphotochem.2023.115012

El-Ghenymy A, Cabot PL, Centellas F, Garrido JA, Rodríguez RM, Arias C, Brillas E (2013) Mineralization of sulfanilamide by electro-Fenton and solar photoelectro-Fenton in a pre-pilot plant with a Pt/air-diffusion cell. Chemosphere 91(9):1324–1331. https://doi.org/10.1016/j.chemosphere.2013.03.005

Fallah Z, Zare EN, Ghomi M, Ahmadijokani F, Amini M, Tajbakhsh M, Arjmand M, Sharma G, Ali H, Ahmad A, Makvandi P, Lichtfouse E, Sillanpää M, Varma RS (2021) Toxicity and remediation of pharmaceuticals and pesticides using metal oxides and carbon nanomaterials. Chemosphere 275:130055. https://doi.org/10.1016/j.chemosphere.2021.130055

Fang K, Zeng X, Yao G, Xia S, Zhao J, Zhou Y, Zhu Y, Li X, Qu C (2023) Wet Oxidation of Pharmaceutical Sludge for the Treatment and Production of Value-Added Materials. Processes 11(9):2747. https://doi.org/10.3390/pr11092747

Fehrenbach GW, Pogue R, Carter F, Clifford E, Rowan N (2022) Implications for the seafood industry, consumers and the environment arising from contamination of shellfish with pharmaceuticals, plastics and potentially toxic elements: A case study from Irish waters with a global orientation. Science of the Total Environment 844:157067. https://doi.org/10.1016/j.scitotenv.2022.157067

Gałązka A, Jankiewicz U, Szczepkowski A (2023) Biochemical Characteristics of Laccases and Their Practical Application in the Removal of Xenobiotics from Water. Applied Sciences 13(7):4394. https://doi.org/10.3390/app13074394

García-Espinoza JD, Robles I, Durán-Moreno A, Godínez LA (2021) Study of simultaneous electro-Fenton and adsorption processes in a reactor containing porous carbon electrodes and particulate activated carbon. Journal of Electroanalytical Chemistry 895:115476. https://doi.org/10.1016/j.jelechem.2021.115476

Gasmi I, Hamdaoui O, Ferkous H, Alghyamah A (2023) Sonochemical advanced oxidation process for the degradation of furosemide in water: Effects of sonication's conditions and scavengers. Ultrasonics Sonochemistry 95:106361. https://doi.org/10.1016/j.ultsonch.2023.106361

Haidar M, Dirany A, Sirés I, Oturan N, Oturan MA (2013) Electrochemical degradation of the antibiotic sulfachloropyridazine by hydroxyl radicals generated at a BDD anode. Chemosphere 91(9):1304–1309. https://doi.org/10.1016/j.chemosphere.2013.02.058

Hammami S, Oturan N, Bellakhal N, Dachraoui M, Oturan MA (2007) Oxidative degradation of direct orange 61 by electro-Fenton process using a carbon felt electrode: Application of the experimental design methodology. Journal of Electroanalytical Chemistry 610(1):75–84. https://doi.org/10.1016/j.jelechem.2007.07.004

Hammami S, Ouejhani A, Bellakhal N, Dachraoui M (2009) Application of Doehlert matrix to determine the optimal conditions of electrochemical treatment of tannery effluents. Journal of Hazardous Materials 163(1):251–258. https://doi.org/10.1016/j.jhazmat.2008.06.124

Hrkal Z, Pastuszek F (2023) Behaviour of PPCP Substances in a Fluvial Aquifer after Infiltration of Treated Wastewater. Applied Sciences 13(16):9348. https://doi.org/10.3390/app13169348

Jiad MM, Abbar AH (2023) Treatment of petroleum refinery wastewater by electrofenton process using a low cost porous graphite air-diffusion cathode with a novel design. Chemical Engineering Research and Design 193:207–221. https://doi.org/10.1016/j.cherd.2023.03.021

Latif W, Ciniglia C, Iovinella M, Shafiq M, Papa S (2023) Role of White Rot Fungi in Industrial Wastewater Treatment: A Review. Applied Sciences 13(14):8318. https://doi.org/10.3390/app13148318

Lin C-C, Huang C-Y (2024) Degradation of sulfamethazine in water in thermally activated persulfate process. Journal of the Taiwan Institute of Chemical Engineers 155:105229. https://doi.org/10.1016/j.jtice.2023.105229

Liu Z, Wardenier N, Hosseinzadeh S, Verheust Y, De Buyck P-J, Chys M, Nikiforov A, Leys C, Van Hulle S (2018) Degradation of bisphenol A by combining ozone with UV and H2O2 in aqueous solutions: mechanism and optimization. Clean Techn Environ Policy 20(9):2109–2118. https://doi.org/10.1007/s10098-018-1595-2

Ljubas D, Juretić H, Badrov A, Biošić M, Babić S (2023) Photocatalytic Degradation of Pharmaceutical Trimethoprim in Aqueous Solution over Nanostructured TiO2 Film Irradiated with Simulated Solar Radiation. Applied Sciences 13(9):5681. https://doi.org/10.3390/app13095681

Mahmoudi N, Farhadian M, Solaimany Nazar AR, Eskandari P, Esfahani KN (2022) Investigation and optimization of the performance of sono-photo-electro-Fenton process for removal of Acid Black 172 and Disperse Blue 56 from polluted water: comparison of the degradation activity with electro-Fenton-based processes. Int J Environ Sci Technol 19(3):1671–1682. https://doi.org/10.1007/s13762-021-03296-0

Mansour D, Alblawi E, Alsukaibi AKD, Al Shammari B (2024a) Removal of Congo red dye by electrochemical advanced oxidation process: optimization, degradation pathways, and mineralization. Sustain Water Resour Manag 10(1):41. https://doi.org/10.1007/s40899-023-01022-x

Mansour D, Alblawi E, Alsukaibi AKD, Humaidi J, Tahraoui H, Shatat M, Teka S, Maisara S, Bellakhal N, Binous H, Amrane A (2024b) Modeling and Optimization of Electrochemical Advanced Oxidation of Clopidogrel Using the Doehlert Experimental Design Combined with an Improved Grey Wolf Algorithm. Water 16(14):1964. https://doi.org/10.3390/w16141964

Mansour D, Alblawi E, Alsukaibi AKD, Lajimi RH, Binous H, Teka S, Bellakhal N, Amrane A (2026) Synergistic Electrocoagulation–Electro-Fenton Coupling for Petroleum Refinery Wastewater Mineralization: Statistical Optimization and Cost Analysis. Processes 14(10):1623. https://doi.org/10.3390/pr14101623

Mansour D, El-Sofany WI, Abdella FaizaIA, Masood N, Khalaf Dhahi Alsukaibi A, Bellakhal N (2021) Doehlert experimental design for the optimization of electrocoagulation treatment of landfill leachate. Environmental Pollutants and Bioavailability 33(1):395–401. https://doi.org/10.1080/26395940.2021.1993752

Mansour D, Fourcade F, Bellakhal N, Dachraoui M, Hauchard D, Amrane A (2012) Biodegradability Improvement of Sulfamethazine Solutions by Means of an electro-Fenton Process. Water Air Soil Pollut 223(5):2023–2034. https://doi.org/10.1007/s11270-011-1002-7

Mansour D, Fourcade F, Huguet S, Soutrel I, Bellakhal N, Dachraoui M, Hauchard D, Amrane A (2014) Improvement of the activated sludge treatment by its combination with electro Fenton for the mineralization of sulfamethazine. International Biodeterioration & Biodegradation 88:29–36. https://doi.org/10.1016/j.ibiod.2013.11.016

Mansour D, Fourcade F, Soutrel I, Hauchard D, Bellakhal N, Amrane A (2015a) Mineralization of synthetic and industrial pharmaceutical effluent containing trimethoprim by combining electro-Fenton and activated sludge treatment. Journal of the Taiwan Institute of Chemical Engineers 53:58–67. https://doi.org/10.1016/j.jtice.2015.02.022

Mansour D, Fourcade F, Soutrel I, Hauchard D, Bellakhal N, Amrane A (2015b) Relevance of a combined process coupling electro-Fenton and biological treatment for the remediation of sulfamethazine solutions – Application to an industrial pharmaceutical effluent. Comptes Rendus Chimie 18(1):39–44. https://doi.org/10.1016/j.crci.2014.05.005

Mathieu D, Nony J, Phan-Tan-Luu R (2000) New Efficient Methodology for Research using Optimal Design (NEMRODW) Software, LPRAI, Univ. Aix-Marseille III, France

Moreira JB, Santos TD, Zaparoli M, De Almeida ACA, Costa JAV, De Morais MG (2022) An Overview of Nanofiltration and Nanoadsorption Technologies to Emerging Pollutants Treatment. Applied Sciences 12(16):8352. https://doi.org/10.3390/app12168352

Mousset E, Loh WH, Lim WS, Jarry L, Wang Z, Lefebvre O (2021) Cost comparison of advanced oxidation processes for wastewater treatment using accumulated oxygen-equivalent criteria. Water Research 200:117234. https://doi.org/10.1016/j.watres.2021.117234

Nikoo M, Regenstein JM, Haghi Vayghan A, Walayat N (2023) Formation of Oxidative Compounds during Enzymatic Hydrolysis of Byproducts of the Seafood Industry. Processes 11(2):543. https://doi.org/10.3390/pr11020543

Oad N, Chandra P, Mohammad A, Tripathi B, Yoon T (2023) MoS2-based hetero-nanostructures for photocatalytic, photoelectrocatalytic and piezocatalytic remediation of hazardous pharmaceuticals. Journal of Environmental Chemical Engineering 11(3):109604. https://doi.org/10.1016/j.jece.2023.109604

Oturan MA (2021) Outstanding performances of the BDD film anode in electro-Fenton process: Applications and comparative performance. Current Opinion in Solid State and Materials Science 25(3):100925. https://doi.org/10.1016/j.cossms.2021.100925

Oturan MA, Aaron J-J (2014) Advanced Oxidation Processes in Water/Wastewater Treatment: Principles and Applications. A Review. Critical Reviews in Environmental Science and Technology 44(23):2577–2641. https://doi.org/10.1080/10643389.2013.829765

Özcan A, Şahin Y, Oturan MA (2013) Complete removal of the insecticide azinphos-methyl from water by the electro-Fenton method – A kinetic and mechanistic study. Water Research 47(3):1470–1479. https://doi.org/10.1016/j.watres.2012.12.016

Panizza M, Cerisola G (2009) Electro-Fenton degradation of synthetic dyes. Water Research 43(2):339–344. https://doi.org/10.1016/j.watres.2008.10.028

Pereira A, De Morais EG, Silva L, Pena A, Freitas A, Teixeira MR, Varela J, Barreira L (2023) Pharmaceuticals Removal from Wastewater with Microalgae: A Pilot Study. Applied Sciences 13(11):6414. https://doi.org/10.3390/app13116414

Puga A, Moreira MM, Figueiredo SA, Delerue-Matos C, Pazos M, Rosales E, Sanromán MÁ (2021) Electro-Fenton degradation of a ternary pharmaceutical mixture and its application in the regeneration of spent biochar. Journal of Electroanalytical Chemistry 886:115135. https://doi.org/10.1016/j.jelechem.2021.115135

Raj S, Manna R, Samanta AN (2024) Spinel ZnMn2O4 nanosphere for the efficient Sulfamethazine degradation under visible light irradiation and photoelectrochemical study. Journal of Environmental Chemical Engineering 12(2):112277. https://doi.org/10.1016/j.jece.2024.112277

Rashmishree KN, Bhaskar S, Shri Hari S, Thalla AK (2023) Correction: Green synthesis of laterite iron-based nanocatalysts using Psidium guajava and Macaranga peltata plant extract for its catalytic application in Fenton's oxidation of triclosan. Clean Techn Environ Policy. https://doi.org/10.1007/s10098-023-02546-8

Ripanda AS, Rwiza MJ, Nyanza EC, Njau KN, Vuai SAH, Machunda RL (2021) A Review on Contaminants of Emerging Concern in the Environment: A Focus on Active Chemicals in Sub-Saharan Africa. Applied Sciences 12(1):56. https://doi.org/10.3390/app12010056

Samir B, Bouazizi N, Nkuigue Fotsing P, Cosme J, Marquis V, Dotto GL, Le Derf F, Vieillard J (2023) Preparation and Modification of Activated Carbon for the Removal of Pharmaceutical Compounds via Adsorption and Photodegradation Processes: A Comparative Study. Applied Sciences 13(14):8074. https://doi.org/10.3390/app13148074

Sigonya S, Mokhothu TH, Mokhena TC, Makhanya TR (2023) Mitigation of Non-Steroidal Anti-Inflammatory and Antiretroviral Drugs as Environmental Pollutants by Adsorption Using Nanomaterials as Viable Solution—A Critical Review. Applied Sciences 13(2):772. https://doi.org/10.3390/app13020772

Sopaj F, Oturan N, Pinson J, Podvorica F, Oturan MA (2016) Effect of the anode materials on the efficiency of the electro-Fenton process for the mineralization of the antibiotic sulfamethazine. Applied Catalysis B: Environmental 199:331–341. https://doi.org/10.1016/j.apcatb.2016.06.035

Suhan MdBK, Shuchi SB, Anis A, Haque Z, Islam MdS (2020) Comparative degradation study of remazol black B dye using electro-coagulation and electro-Fenton process: Kinetics and cost analysis. Environmental Nanotechnology, Monitoring & Management 14:100335. https://doi.org/10.1016/j.enmm.2020.100335

Suleiman M, Demaria F, Zimmardi C, Kolvenbach BA, Corvini PF-X (2023) Analyzing microbial communities and their biodegradation of multiple pharmaceuticals in membrane bioreactors. Appl Microbiol Biotechnol 107(17):5545–5554. https://doi.org/10.1007/s00253-023-12677-z

Tao N, Tian Y, Wang J, Teng J (2025) Enhanced electrochemical removal of sulfamethazine on Sm-doped Ti4O7 anode: Mechanisms and toxicity evaluation. Journal of Hazardous Materials Advances 17:100607. https://doi.org/10.1016/j.hazadv.2025.100607

World Health Organization (2012) World health statistics 2012. Statistiques sanitaires mondiales 2012 :176

Yin Y, Xu H, Zhu Y, Zhuang J, Ma R, Cui D, Jiao Z (2023) Recent Progress in Applications of Atmospheric Pressure Plasma for Water Organic Contaminants' Degradation. Applied Sciences 13(23):12631. https://doi.org/10.3390/app132312631

Zhang Q, Zhou M, Du X, Su P, Fu W, Song G (2022) Highly efficient dual-cathode Electro-Fenton process without aeration at a wide pH range: Simultaneously enhancing Fe(II) regeneration and mineralization efficiency. Chemical Engineering Journal 429:132436. https://doi.org/10.1016/j.cej.2021.132436